XL CILAMCE
IBERO-LATIN AMERICAN CONGRESS ON COMPUTATIONAL METHODS IN ENGINEERING
NOVEMBER 11-14, 2019
Praiamar Natal Hotel & Convention Natal, RN-BRAZIL

BINARY SHADING CLASSIFICATION BY MEANS OF AN IDENTIFICATION ALGORITHM FOR RADIATION TRANSITIONS USING LOW COST SENSORS

Felipe P. Marinho
Juarez P. Amorim
Juliana S. Brasil
Jonathan B. Araújo
Paulo A. C. Rocha
Maria E. V. Silva
Ricardo J. P. Lima
felipe.pinto.marinho@gmail.com
juarezneto33@hotmail.com
julianasbra@gmail.com
barroso26jonathan@gmail.com
paulo.rocha@ufc.br
eugenia@ufc.br
rjponteslima@gmail.com
Mechanical Engineering Department, Technology Center, Federal University of Ceará
Campus do Pici, 60440-593, Ceará, Brazil

Abstract. In the current energy scenario, renewable energies such as solar and wind power have significant relevance. In this context, an algorithm capable of recognizing irradiation transitions was implemented. This algorithm was used to classify data obtained from light dependent resistance in two classes: shadow and non-shadow. These results were compared with those obtained by a standard algorithm that has a input global or beam irradiation values collected by pyranometer and pyreliometer sensors, respectively. This way, a practical tool was obtained. Such tool uses data collected by low cost sensors to perform an initial statistical study about days and hours when there is a higher level of irradiation. Therefore, this information can be used to optimize the solar power capture. The irradiation transition identification algorithm, generally, had a better compilance at peaks hours, where for the same days it reached ranging around 100% and 87.10% using the global and beam components as input to the standard algorithm, respectively. From the results, it is clears that a better performance of the irradiation transition identification algorithm when using global irradiation values as input to the standard algorithm, as well as a lower compilance of the irradiation transition algorithm during the dawn and twilight periods.

Keywords: Beam irradiation, Global irradiation, Irradiation identification algorithm, Standard algorithm.

1 Introduction

The need to use renewable sources of energy, which are less polluting than the fossils ones, is one of the main tendency of today's society and solar energy is an outstanding alternative. However, the intermittent character of the solar resource is characterized as a barrier to more significant amount of solar plant installations Inman, Pedro and Coimbra [1]. In addition, it is known that the level of luminosity affects the productivity and quality of plants crops, such as heliconia psittacorum Silva et al. [2]. Forecast methods for solar irradiation may also provide estimates of solar irradiance to determine evapotranspiration levels estimated by solar radiation method Duarte et al. [3]. The intensity of insolation, a parameter related to solar irradiation, is relevant in the analysis of pasture quality Passos et al. [4]. All these studies show the importance of having methods that provide greater knowledge about the solar resource. In this context, several methods of forecasting irradiation values have been developed, some of them using machine learning algorithms Larsson and Coimbra [5]. Pedro and Coimbra [6,7]. Pedro et al. [8]. Others perform analysis on the time series of irradiation Dong et al. [9]. Trapero, Kourentzes and Martin [10] and there are also those working with the identification of irradiation transitions Chu et al. [11]. Lappalainen e Valkealahti [12]. The objective of this study was to implement an irradiation transition identification algorithm (ITIA) Lappalainen e Valkealahti [12] that was used to classify data provided by light dependent resistor (LDR) sensors in two classes: shadow and non-shadow. The results were compared with those obtained by standard algorithm that uses irradiation data obtained by pyranometer and pyreliometer sensors, where the performance of ITIA could be evaluated.

2 Methodology

2.1 Data Collect

The data of the global component of solar irradiation were obtained in Fortaleza, CE, with a sampling frequency of 1 measurement each 2 seconds. However, the values considered were means obtained for 2 minutes collection, using a pyranometer, since beam component of the solar irradiation was collected by an analogous procedure, differing only by the use of a pyreliometer. Measurements were performed at intervals of 1 hour in the range of 10h00 to 16h00. For example, from 10h00 to 11h00, 11h00 to 12h00, and so on, for the months of June, July, August and September of the year 2016. The interval from 13h00 to 14h00 was removed due to the presence of noisy values (such as negative values irradiation, arising from a problem in the sensor) in the month on June, so consistency of the results could be guaranteed. The data for that same interval of the other months were also disregarded. These irradiance values were implemented into the standard algorithm, which was used to evaluate the performance of the proposed model. The ITIA input consists of values provided by LDR sensors that were connected to a microcontroller with built in input/output support for data acquisition, with a sampling frequency of 1 measurement per second in the same period of collection of the irradiation data.

2.2 Irradiation Transition Identification Algorithm

For its operation, the algorithm receives the data obtained by the LDR sensors so it can perform calculations of moving averages in dataset, f_x, based on 5 elements. Let $X=\{x_1, x_2, \ldots, x_n\}$ be the set of values, x_n, given by the brightness sensors, it follows that the moving averages obtained from X are given by Eq. (1), (2) and (3).

$$f_1 = \frac{(x_1+x_2+x_3+x_4+x_5)}{5}. \quad (1)$$

$$f_2 = \frac{(x_2+x_3+x_4+x_5+x_6)}{5}. \quad (2)$$

by recurrence,

$$f_{n-4} = \frac{(x_{n-4}+x_{n-3}+x_{n-2}+x_{n-1}+x_n)}{5}. \quad (3)$$

The next step is to determine the variances for successive moving averages, q_x. This procedure is represented by Eq. (4), (5) and (6).

$$q_1 = f_2 - f_1. \quad (4)$$

$$q_2 = f_3 - f_2. \quad (5)$$

again by recurrence

$$q_{n-5} = f_{n-4} - f_{n-5}. \quad (6)$$

The next step of the algorithm is to compare these variations with a limit value (VL). For the work in question, VL = 5, Lappalainen e Valkealahti [12].

- If $q_k \geqslant VL$, then the non-shadow class;
- if $q_k \leq -VL$, then the shadow class;
- if $-VL < q_k < VL$, there is non-transition, so the previous class remains.

2.3 Parametrization Procedure

Note that the sampling frequency of the input of the standard algorithm is different from the sampling frequency of the ITIA input. Therefore, it was necessary to develop a parametrization procedure to make the number results provided by ITIA equivalent to that provided by standard algorithm, thus allowing the confrontation of these results and concluding about the accuracy of the ITIA. The basic idea was to establish a grouping criterion, where for each irradiation value collected, a group of LDR data would correspond, in which ITIA was applied to obtain result.

Let the sets A={a_1, …, a_n} and B={b_1, …, b_m} of LDR and irradiance data, respectively. For each set corresponds the collections D={d_1, …, d_n} and E={e_1, …, e_m} the instants where they were obtained. Then, as an example, taking the jth element of the set D, d_j, this represents the time instant at which a_j was collected. The next step was to convert the times that were represented by hour, minute and second into real numbers, this was easily accomplished using numerical programming software. If d_j belongs to the interval [e_i - ε, e_i + ε] then a_j is part of the C_i group, for values of j varying in the list {1, ..., n} and for i fixed, after all these comparisons the i is incremented and the process is repeated. At the end of this step, m data groups of the LDR are generated, so that given b_K one has the corresponding group C_K. Where ε = 0.0006944, which is the value assigned for the 1 minute interval by the software used for the implementations.

2.4 Standard Algorithm

The algorithm receives the data supplied by the pyranometer or the pyreliometer, with which it computes the clear sky index Kt, given by Eq. (7).

$$k_t = \frac{I}{I_o}(n,t). \quad (7)$$

at where,

I : Beam or Global component of irradiation at time t and day n

I_o : extraterrestrial irradiation at time t and day n

For the calculations of I_o, geometrics considerations were used Duffie and Beckman [13]. With the values of k_t, it has been:

- If$k_t < L$, then the shadow class;
- If $k_t \geqslant L$, then the non-shadow class.

L: a variable limit value, whose influence has been assessed.

2.5 Confusion Matrix

To confront the results, we used a confusion matrix, which consists of a square matrix of order equal to the number of classes involved in the problem. In this work, as it is a problem of two classes, the matrix will have structure as shown in Table 1.

Table 1. Confusion matrix

Criterion	Non-shadow$_{ITIA}$	Shadow$_{ITIA}$
Non-shadow$_{P}$	X	Y
Shadow$_{P}$	Z	U

Where the subscripts P and ITIA indicate the results provided by the standard algorithm and the ITIA, respectively.
X = Number of hits, where the standard algorithm and ITIA provided non-shadow, as a result.
Y = Number of errors, where the standard algorithm and ITIA provided non-shadow and shadow, respectively.
Z = Number of errors, where the standard algorithm and ITIA provided shadow and non-shadow, respectively.
U = Number of hits, where the standard algorithm and ITIA provided shadow, as a result.
Therefore, the percentage of ITIA hit is given by Eq. (8).

$$\eta = \frac{(X+U)}{(X+Y+Z+U)}. \tag{8}$$

3 Results and Discussion

The Tables 2 and 3, show the percentages of average hits for the classification, using the global component and beam component, respectively, as input for the standard algorithm considering the measurement months for certain values of L.

Table 2. Mean percentages for the global component as input to the standard algorithm

	L=0.3	L=0.4	L=0.5	L=0.6	L=0.7	Standard deviation
June	54.84%	61.29%	66.45%	65.81%	59.35%	0.0480
July	58.06%	50.97%	51.61%	57.42%	63.35%	0.0511
August	61.38%	55.74%	59.89%	54.62%	56.56%	0.0287
September	61.08%	63.02%	55.28%	46.89%	46.61%	0.0769

Table 3. Mean percentages for the beam component as input to the standard algorithm

	L=0.3	L=0.4	L=0.5	L=0.6	L=0.7	Standard deviation
June	57.42%	56.13%	49.68%	47.74%	49.03%	0.0444
July	45.16%	45.16%	45.16%	44.51%	43.22%	0.0084
August	63.44%	37.66%	29.85%	31.23%	37.85%	0.1360
September	36.44%	34.41%	33.04%	34.32%	34.33%	0.0122

These results are summarized in Fig. 1 and 2.

By the analysis of Tables 1 and 2, it is possible to notice that ITIA has a better performance when the input of standard algorithm are the values of the global irradiance component when compared to the input of beam irradiation, a fact verified in the works Pedro and Coimbra [7], Trapero, Kourentzes and Martin [10]. In Pedro et al.[8] it was also noted that the beam irradiation predictions are less reliable than the corresponding ones for the global component.

The Fig. 3, 4, 5 and 6, illustrate the variation of the mean percentages of correctness during the day, when the input of the standard algorithm are values of global irradiation. In the case where the input consists of beam irradiation, the behavior is similar, and it is worth noting that the results obtained for the interval of 13h00 to 14h00 were not considered, due to the presence of noisy data in June. In order

to guarantee consistency in the results, the data for that same time interval of the other months were disregarded.

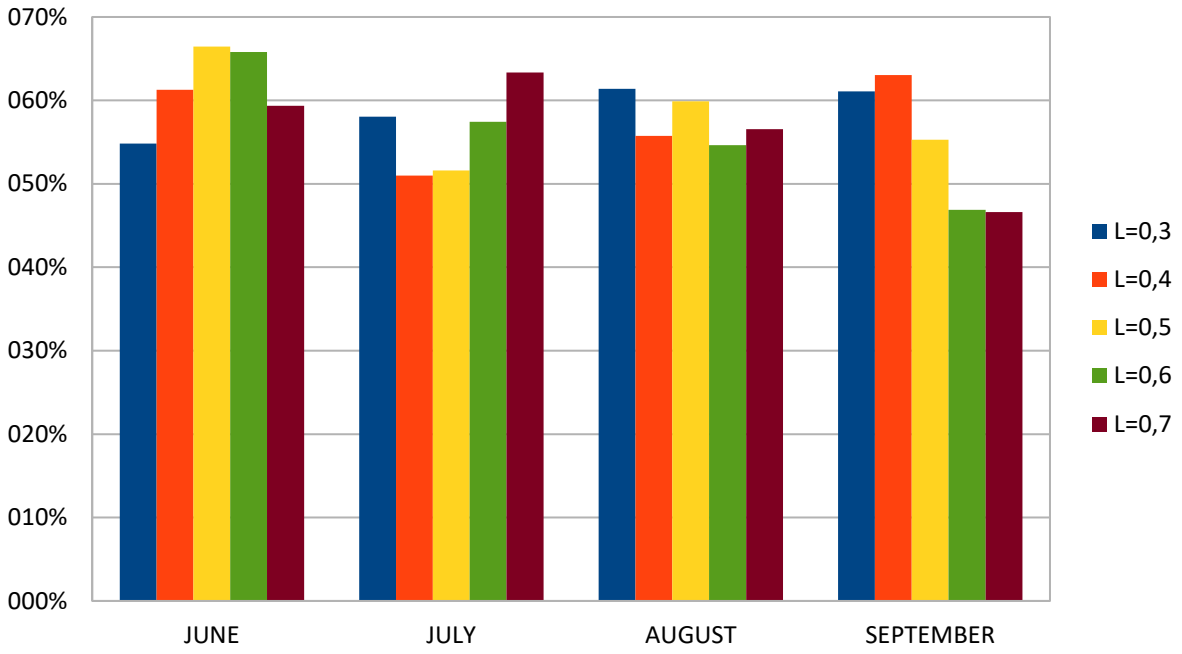

Figure 1. Mean percentages for the global component as input to the standard algorithm

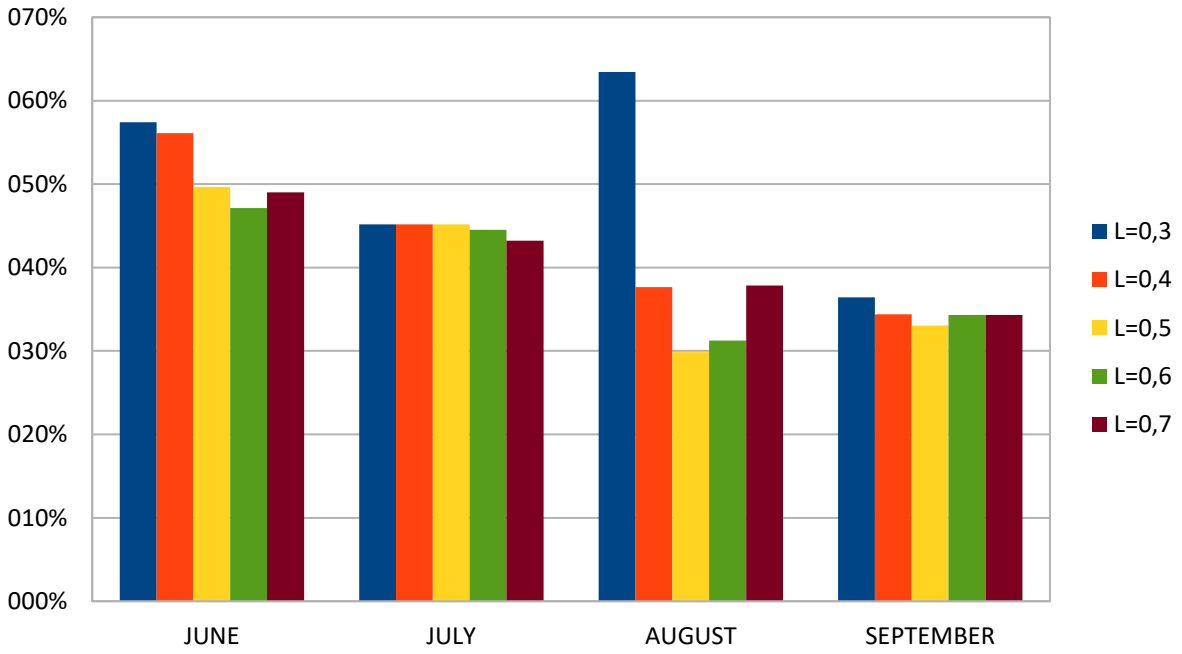

Figure 2. Mean percentages for the beam component as input to the standard algorithm

Evaluating the Fig. 3, 4, 5 and 6, it is noticed that ITIA generally has better compliance with the standard algorithm at peak of 11h00 to 15h00 hours, except for July, this being justified by data of this month present a greater variability. In fact, variability in the data tends to cause lower levels of accuracy for some algorithms, as perceived in Pedro and Coimbra [7], Nonnenmachter, Kaur and Coimbra [14], Aryaputera, Yang and Walsh [15]. For the start and end bands of the day, ITIA presented lower mean percentages, which is expected since these periods are characterized by being the decision boundaries

of the problem and classification algorithms usually show reduction in their performance in those regions. In addition, the values collected by the LDR sensors in these bands are still high, while the irradiation provided by the pyreliometer and pyranometer sensors is low, indicating a sensitivity problem of the LDR sensors. For later studies, the increase of the sensitivity of the LDR sensors will be obtained by the addition of filters of lenses and changes in the electrical circuit of the acquisition system. This reduction in the accuracy of ITIA at start and end of the day is not critical, as the greater interest is in the classification at peak times, since it is at those periods when the greatest availability of the solar resource occurs. For this track, the ITIA showed good compliance with the standard algorithm.

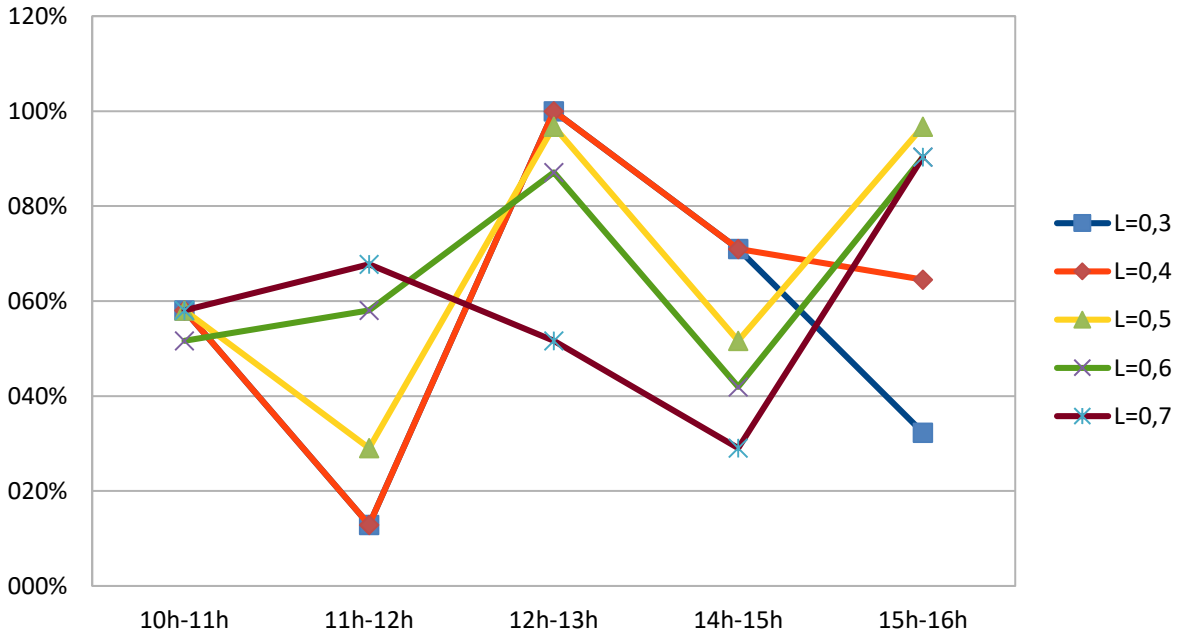

Figure 3. Variation of mean percentages of correctness throughout the day for the month of June

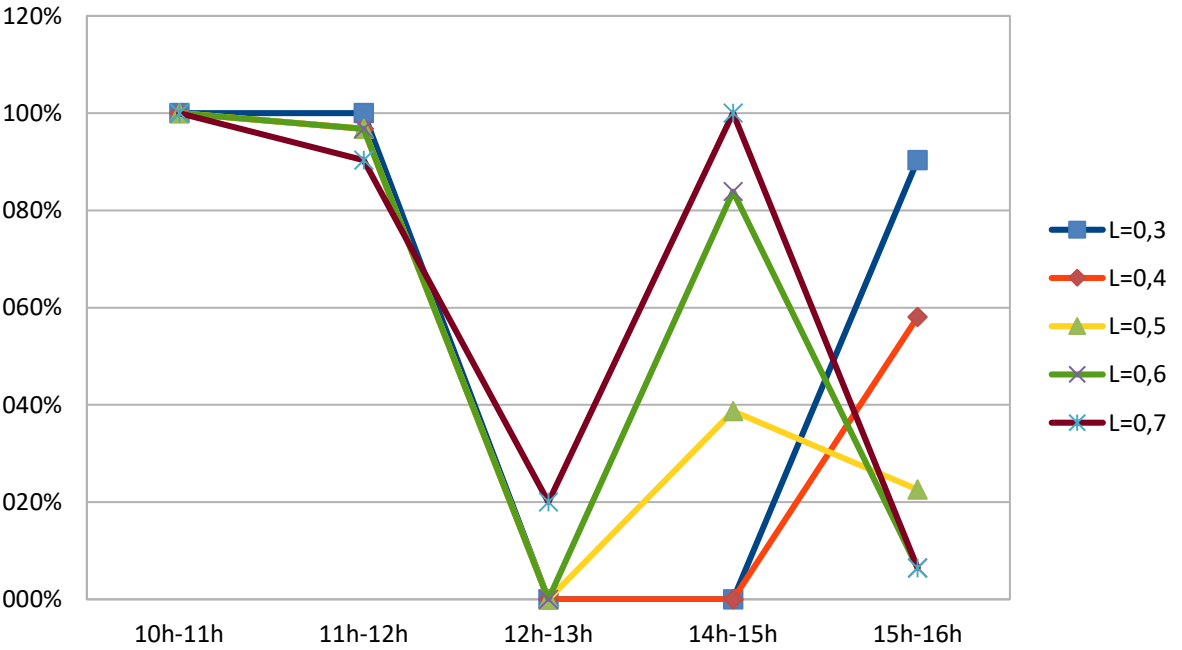

Figure 4. Variation of mean percentages of correctness throughout the day for the month of July

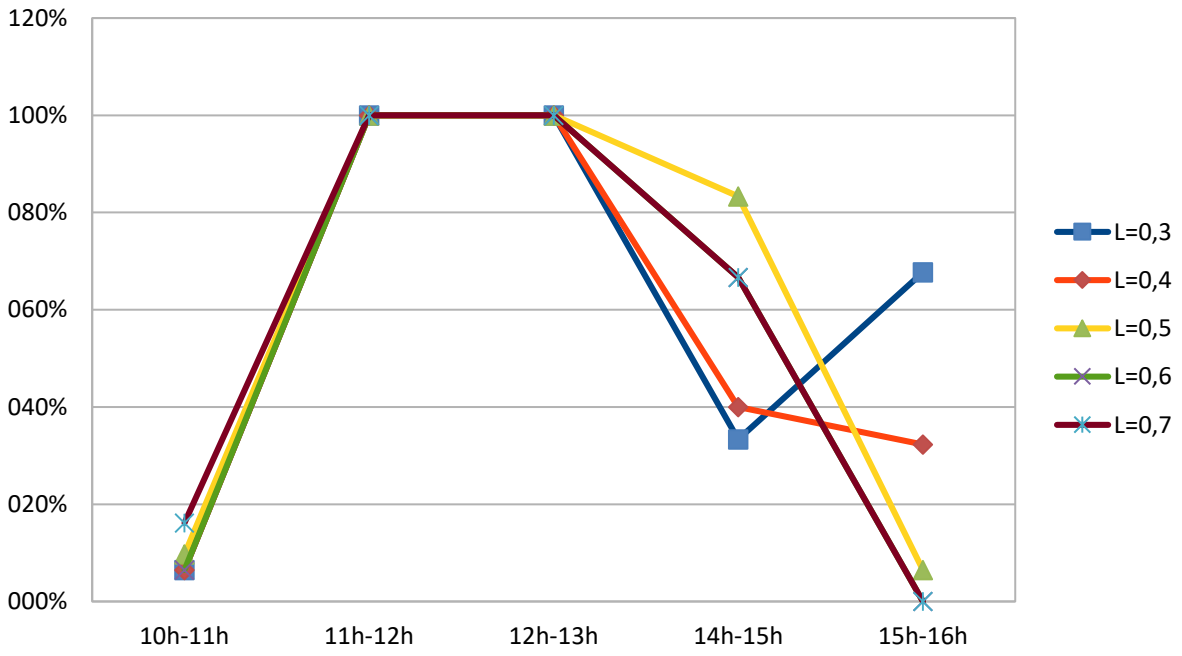

Figure 5. Variation of mean percentages of correctness throughout the day for the month of August

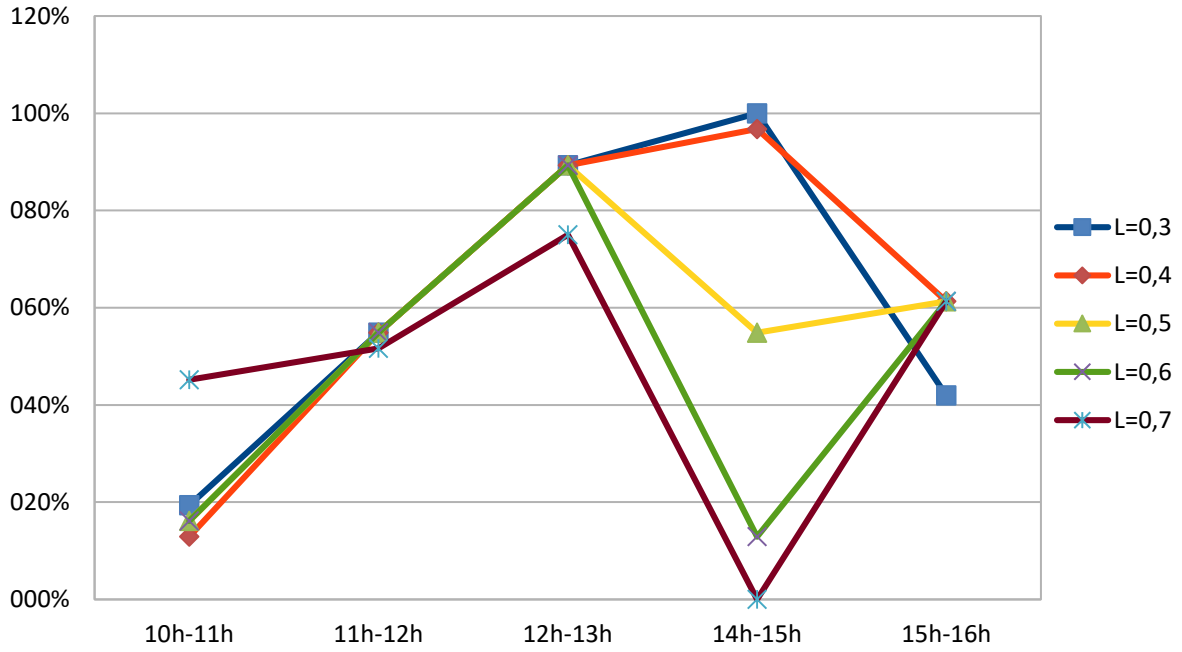

Figure 6. Variation of mean percentages of correctness throughout the day for the month of September

Conclusion

The work developed in this paper, sought the implementation of an algorithm of identification of transitions of irradiation to perform the classification of data obtained by LDR sensors in two classes: shadow and non-shadow. These results were compared with those obtained by a standard algorithm that

uses as inputs global and beam components of irradiation. This way, the following conclusions could be obtained:

1. ITIA performed poorly for the performance of shading classifications when compared to its performance in identifying irradiation transitions.
2. By the analysis of the results, it is noticed that the percentages of correctness of the AITI were generally higher when using values of the global component of irradiation as input to the standard algorithm.
3. Except for July, ITIA performance was generally worsened at the start and end of the day, which is probably due the fact that the irradiance values are milder, while the brightness data are already high and because of these periods being the decision boundaries of the problem.

After making certain adaptations in the acquisition process, it is believed that there will be significant improvement in the accuracy of the ITIA, thus providing a practical tool to carry out analyzes that will provide information about the solar potential of a certain region, using as input values obtained by lower cost sensors.

Acknowledgements

This research was supported by the Coordenação de Aperfeiçoamento de Pessoal de Nível Superior (CAPES) and the Conselho Nacional de Desenvolvimento Científico e Tecnológico (CNPq), Brazilian governmental agencies.

References

[1] R.H. Inman, H.T.C. Pedro and C.F.M. Coimbra. Solar forecasting for renewable energy integration. *Progress in energy and combustion science*, vol. 39, pp. 535–576, 2013.
[2] M.W. Silva. E.O. Ono, M.H.L.C. Santos, M.Z.B. Cavalcante, G.M. Oliveira, D.N.C. Ferreira and C.C. Lopes. Growth and production of heliconia under different light conditions. *Semina: Ciências Agrárias*, vol. 38, pp. 7–18, 2017.
[3] G.R.B. Duarte, E.R. Schoffel, M.E.G. Mendez and V.A. Paula. Measure and estimation of the evapotranspiration of tomato plants cultivated with organic fertilization in protected ambient. *Semina: Ciências Agrárias*, vol. 31, pp. 563–574, 2010.
[4] R.R. Passos, L.M. Costa, D.L. Burak and D.A. Santos. Indicadores da qualidade de pastagens degradadas sob condições de relevo acidentado. *Semina: Ciências Agrárias*, vol. 36, pp. 2465–2482, 2015.
[5] D.P. Larsson and C.F.M. Coimbra. Direct power output forecasts from remote sensing image processing. *Journal of solar energy engineering*, vol. 140, 2018.
[6] H.T.C. Pedro and C.F.M. Coimbra. Short-term irradiande forecastability for various solar micro-climates. *Solar Energy*, vol. 122, pp. 587–602, 2015.
[7] H.T.C. Pedro and C.F.M. Coimbra. Nearest-neighbor methodology for prediction of intra-hour global horizontal and direct normal irradiances. *Renewable Energy*, vol. 80, pp. 770–782, 2015.
[8] H.T.C. Pedro, C.F.M. Coimbra, M. David and P. Lauret. Assessment of machine learning techniques for deterministic and probabilistic intra-hour solar forecasts. *Renewable Energy*, vol. 123, pp. 191–203, 2018.
[9] Z. Dong, D. Yang, T. Reindl and W.M. Walsh. Short-term solar irradiance forecasting using exponential smoothing state space model. *Energy*, vol. 55, pp. 1104–1113, 2013.
[10] J.R. Trapero, N. Kourentzes and A. Martin. Short-term solar irradiation forecasting based dynamic harmonic regression. *Energy*, vol. 84, pp. 289–295, 2015.
[11] Y. Chu, H.T.C. Pedro, M. Li and C.F.M. Coimbra. Real-time forecasting of solar irradiance ramps with smart image processing. *Solar Energy*, vol. 114, pp. 91–104, 2015.
[12] K. Lappalainen and S. Valkealahti. Recognition and modelling of irradiance transitions caused by moving clouds. *Solar Energy*, vol. 112, pp. 55–67, 2015.

[13] J.A. Duffie and W.A. Beckman. Solar engineering of thermal process. *John Wiley & Sons*, New Jersey, 2013.
[14] L. Nonnenmachter, A. Kaur and C.F.M. Coimbra. Day-ahead resource forecasting for concentrated solar power integration. *Renewable Energy*, vol. 86, pp. 866–876, 2016.
[15] A.W. Aryaputera, D. Yang and W. M. Walsh. Day-ahead solar irradiance forecasting in a tropical environment. *Journal of Solar Energy Engineering*, vol. 137, 2015.